Lithospheric inversions and the assimilation of complementary information: Some examples relevant for EarthScope

M.H. Ritzwoller and N.M. Shapiro

University of Colorado at Boulder, Boulder, CO 80309-0390 (ritzwoller@ciei.colorado.edu)

Summary

Application of complementary data sets to improve the understanding of the U.S. lithosphere is a defining characteristic of EarthScope. We discuss the joint inversion of surface wave dispersion with heat flow data and receiver functions (RFs). Heat flow data, in particular, help to reduce the range of acceptable seismic models and improve the inference of temperature and compositional variations. Multiple spatial scales of sensitivity make assimilation of RFs difficult, which USARRAY will help address if stations will be installed long enough to extract meaningful and reliable RFs.

1. Introduction

Observations of surface wave dispersion provide more or less spatially continuous constraints on the lithosphere across the United States and, indeed, across much of the globe. In contrast with surface waves, most other types of information are spatially discrete (e.g., heat flow measurements, receiver functions, teleseismic travel times). Therefore, shear velocity models of the crust and uppermost mantle derived predominantly from observations of the dispersion of surface waves can be fruitfully thought of as the framework or large-scale context in which to introduce a wide variety of geophysical information in the attempt to model and understand the North American lithosphere.

We discuss the assimilation of two types of information in the context of surface wave inversions to improve models of the continental lithosphere: heat flow data and receiver functions. Receivers functions are sensitive to sharp boundaries in and around the crust and, therefore, provide important constraints on crustal structure. Heat-flow data constrain mantle shear velocities through the conversion of heat-flow into temperature and subsequently into shear velocity at the top of the upper mantle. Our principal purpose is to discuss how these constraints, in particular, improve the estimated seismic model and also lead to better inferences of temperature and composition.

We note two key challenges in assimilating disparate data in the context of a surface wave inversion. The first is the problem of multiple spatial scales of sensitivity. For example, receiver functions provide information about structures averaged over ten or several tens of kilometers beneath the receiver. Surface wave models are on a larger scale. Assimilating information from receiver functions over a broad region, therefore, requires fairly good station coverage which, at present, does not exist except in a very small fraction of the U.S. (e.g., parts of S. California). Clearly, USARRAY will facilitate this if stations are installed long enough to extract reliable receiver functions. A second challenge in successfully assimilating data is acquiring and using meaningful uncertainty estimates in all quantities. This is particularly important in the assimilation of heat flow data.

In the following, we will: provide a brief overview of the state of our work to map surface wave dispersion and lithospheric shear velocities across the U.S., discuss efforts to infer lithospheric temperature from shear velocities and interpret the results in terms of a simple thermal model of the uppermost mantle, and discuss how assimilating heat flow data and receiver functions reduces uncertainties and improves the vertical resolution of the seismic and thermal models.

2. Lithospheric inversion with surface wave dispersion alone

Improvements in station coverage, greater breadth of the frequency band of measurements (e.g., 15 s - 200 s globally), the construction and use of better starting models of the crust (e.g., CRUST5.1 of Mooney and collaborators; CRUST2.0, Laske pers. comm., 2001), and advances in data processing and inversion methodologies are combining to improve global shear velocity models of the crust and uppermost mantle. Figure 1 shows dispersion maps and model shear velocities directly beneath the Moho that exemplify the current state of affairs. The primary data-set used to construct the shear velocity model consists of broad-band Rayleigh and Love wave group-velocity (CU-Boulder; e.g., Ritzwoller and Levshin, 1998) and phase-velocity (Harvard, Utrecht Universities; Ekström *et al.*, 1997; Trampert and Woodhouse, 1995) dispersion curves. The dispersion maps result from a new method of surface wave tomography called "diffraction tomography" that is based on a physical model of the surface wave Fresnel zone rather than on ray-theory and ad hoc regularization such as the method documented by Barmin *et al.* (2001).

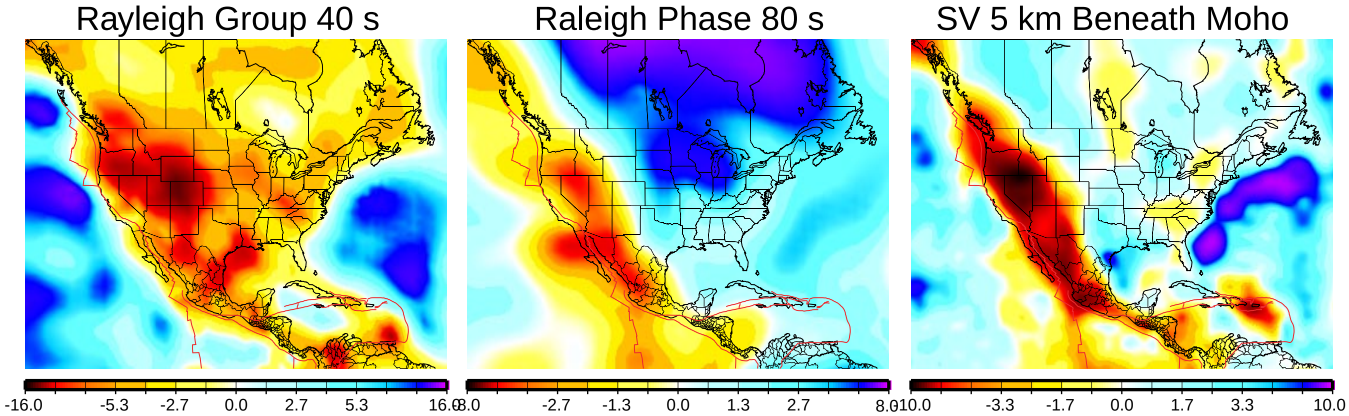

Figure 1: Examples of Rayleigh wave dispersion maps and v_{sv} speed in the uppermost mantle. Maps are presented as a percent perturbation to a reference value: PREM velocities for the dispersion maps and the global average velocity 5 km beneath Moho for the v_{sv} map. Group velocity data are from CU-Boulder and phase velocity data are from Harvard and Utrecht Universities. The v_{sv} velocities are taken from the center of the ensemble of acceptable models.

Diffraction tomography accounts for path-length dependent sensitivity, wave-form healing and associated diffraction effects, and provides a more accurate assessment of spatially variable resolution than traditional tomographic methods. The shear velocity model derives from a Monte-Carlo inversion of the dispersion maps for an ensemble of acceptable shear velocity models of the crust and uppermost mantle (Shapiro and Ritzwoller, 2001).

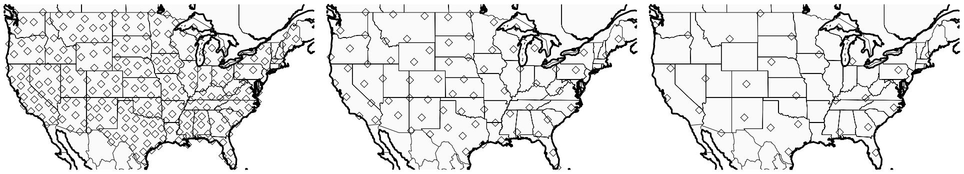

Figure 2: Hypothetical station coverage for the USARRAY reference network with station spacings of 150km, 300 km, and 500 km.

Results such as those in Figure 1 would be greatly improved by using data from USARRAY. To estimate the resolution that might result from the reference network component of USARRAY, we performed simulations for a variety of station coverages such as those shown in Figure 2. We assumed data acquisition for 4 years, with synthetic measurements for events satisfying a reasonable distance:magnitude criterion observed only at stations within the conterminous United States. The method of resolution analysis is described by Barmin *et al.* (2001), but here we report results from diffraction tomography. The resulting resolution estimates averaged over the entire U.S. are shown in Figure 3 for five different station spacings. The spacing of the tomographic grid is 111 km, so maximum resolution is 222 km. On average, resolution degrades with period because Fresnel zones widen. To a fair approximation, at long periods the resolution will be somewhat less than the interstation spacing but at periods below about 50 s the expected resolution may approach half the interstation spacing. Thus, for example, to obtain a 100 km resolution with surface waves, a 200 km station spacing may suffice if the network operates long enough, except at long periods.

3. Inferring temperature from shear velocity

We use the method by Goes et al. (2001) to infer the temperature distribution in the upper mantle from the shear velocity model. Isotropic shear-velocities are converted to temperatures based on laboratory measured thermoelastic properties of mantle minerals and the average mineralogical composition of the mantle beneath different tectonic provinces. In particular, we assume that the mantle is composed of five principal minerals: olivine, orthopyroxene, clinopyroxene, spinel, and garnet. For each mineral, we calculate the shear modulus and the density as functions of temperature, pressure, and iron content based on laboratory-observed derivatives (e.g., Goes et al., 2001). The

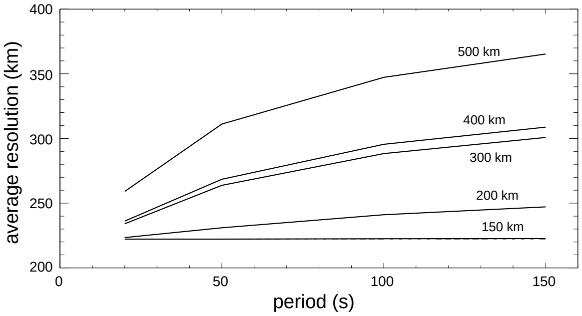

Figure 3: Estimated hypothetical resolution averaged across the conterminous United States as a function of period, plotted for different hypothetical station spacings. The theoretical limit in this simulation is 222 km.

average shear modulus and density for a given mantle composition are calculated based on volumetric proportions of individual minerals and the Voigt-Reuss-Hill averaging scheme. After applying the relation $\beta = \sqrt{\mu/\rho}$ and introducing corrections for anelasticity, we obtain the average shear velocity as a function of iron content, mineralogical composition, temperature, and depth (actually pressure, but we neglect lateral pressure variations).

At each geographical location, we fix the mineralogical composition based on compositional models of the mantle beneath different tectonic provinces (McDonough and Rudnick, 1998). In most locations, the iron content can be considered constant with depth. However, beneath cratons this assumption leads to implausible temperature profiles with an aphysical temperature minimum in the lithosphere. As Figure 5 shows later, this feature can be removed if the uppermost mantle is slightly depleted in iron. After fixing the composition, the shear velocity at each depth depends only on temperature, and an optimal temperature at each depth can be found with a grid search.

4. Assimilation of heat flow data

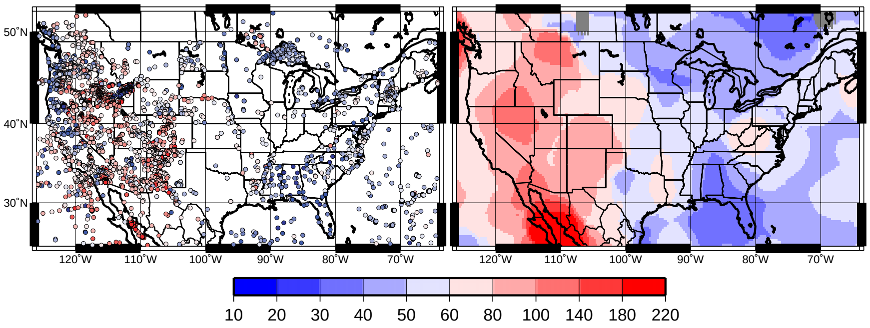

Figure 4: (LEFT) Heat flow observations taken from the data base compiled by Pollack*et al.* (1993). (RIGHT) Smoothed version of the data set with no data rejection. Units are mW/m^2.

Assimilation of heat flow data in a surface wave inversion is relatively straightforward for two reasons. First, as Figure 4 illustrates, heat flow measurements already may be sufficiently dense over much of the U.S. to allow the construction of a smooth map with a resolution similar to surface wave maps. However, over much of the central part of North America heat flow measurements are not very dense and a more careful analysis by experts may necessitate rejecting many of the measurements in the data base shown in Figure 4. It would be useful if a significant initiative within EarthScope would be the construction of an updated heat flow map for the United States with associated information. Second, heat flow neatly constrains temperatures and, hence, shear velocities near the top of the mantle where surface wave inversions are beset with particularly strong trade-offs. The vertical gradient in the uppermost mantle is hard to determine reliably with surface wave data alone. This is made possible by the fact that, to a fair approximation, the crustal temperature gradient can be considered linear. The major caveats are that radioactive heat generation in the crust is poorly known and the inference of temperature at the top of the mantle requires a knowledge of depth to Moho. The first caveat requires that heat flow measurements corrected for crustal radioactive heat generation must be accompanied by error estimates that incorporate uncertainties in crustal-generated heat. The second caveat can be overcome in the simultaneous inversion because Moho depth is a free variable in the inversion.

Figure 5 presents examples of inversions with and without the assimilation of heat flow data at a point in the Canadian shield. This procedure currently is under development, but there are four features worth particular note. (1) The application of the heat flow constraint reduces the range of acceptable shear velocity models in the uppermost mantle. (2) It also produces more realistic temperature profiles from the shear velocity which, under cratons, can exhibit aphysical temperature minima in the uppermost mantle if the constraint is not applied. (3) The linearity of the temperature gradient with depth is clarified under cratons if the uppermost mantle is slightly depleted in iron. (4) The thermal lithosphere can be identified as the region of intersection between the linear conductive uppermost mantle and the adiabatic deep mantle. Much further work is needed to incorporate uncertainties in all quantities (heat flow measurements, crustal radioactive heat generation, mantle composition, etc.) in the inference of temperature. Our efforts are largely based on the uppermost mantle temperature model of Artemieva and Mooney (2001).

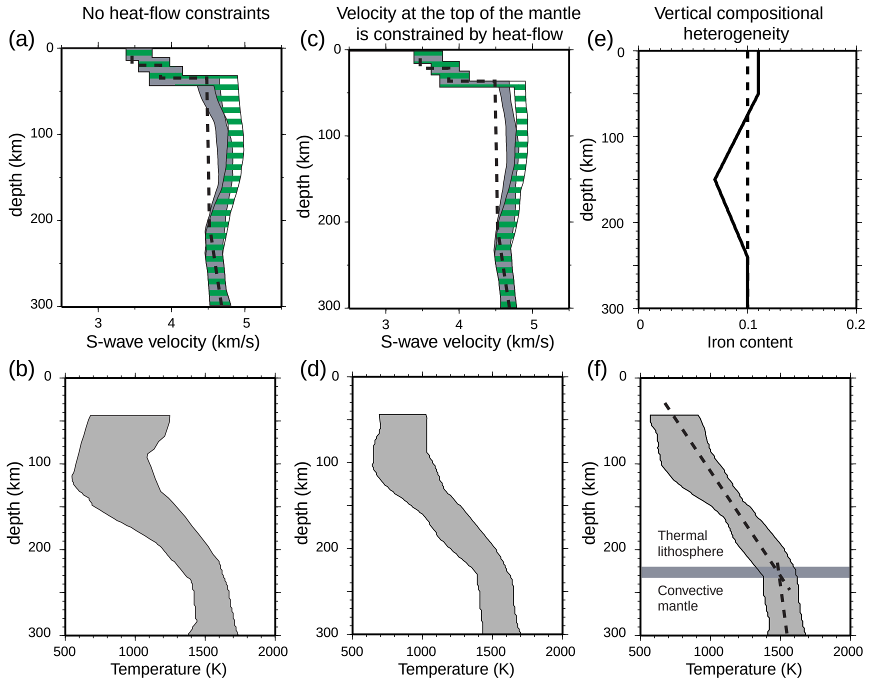

Figure 5: Examples of inversions with and without the heat flow constraint for a point in the Canadian shield (52N, 90W). (a) Ensemble of acceptable radially anisotropic shear velocity models produced from surface wave dispersion alone. Hatched regions are v_{sh} and grey-shaded regions are v_{sv} in the mantle. (b) Ensemble of temperature models derived from v_s in (a). (c) Shear velocity model produced when heat flow data are included in the inversion. For reference, the dashed line in (a) and (c) is from a global 1-D model. (d) Temperature profiles derived from (c). (e) Dashed lines show mantle Fe content used to construct (b) and (d). Solid line, with lithospheric Fe depletion, is used to construct (f). (f) Ensemble of temperature profiles with a depleted mantle in which surface wave and heat flow data are fit simultaneously. The linear gradient overlying the mantle adiabat defines the thermal lithosphere.

5. Assimilation of receiver functions

Receiver functions (RF) provide information complementary to heat flow, in that they constrain crustal structures. Their use in conjunction with surface waves has been explored by other researchers (e.g., Julia *et al.*, 2000). Figure 6 shows that in some parts of the U.S. our shear velocity model is consistent with observed RFs (e.g., beneath station PFO), but in other areas there is striking disagreement (e.g., station ANMO). In the latter case the joint inversion of surface waves with RFs changes the mantle part of the model appreciably.

We close this discussion by noting that RFs may vary strongly with azimuth, and further efforts are needed to optimize the way RFs are included in inversions with surface wave data. Our experience is that RFs are most useful for stations operating for a long time so that the azimuthal variations are well constrained and understood.

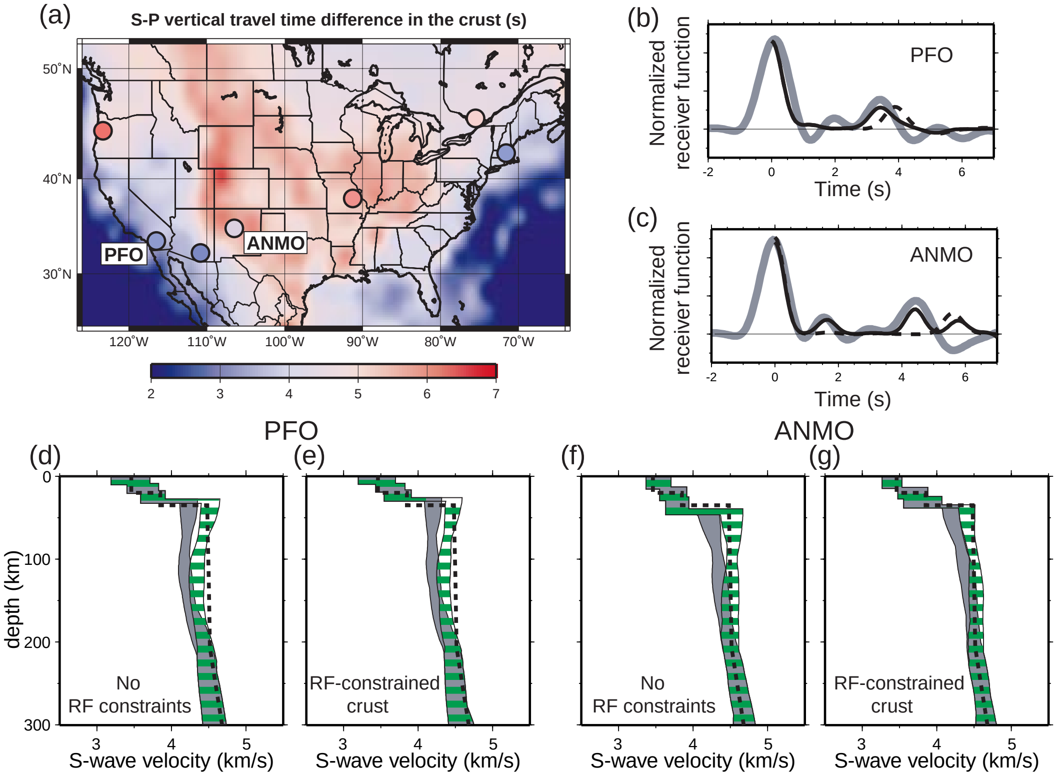

Figure 6: The effect of assimilating receiver functions (RF) in shear velocity inversions. (a) Maps of $S - P$ vertical travel times in the crust predicted by our shear velocity model. Colored circles show the $S - P$ times estimated from RFs at several stations. (b) RF example for station PFO. Gray line is the observed RF, solid and dashed black lines are the RFs predicted from the shear velocity with and without the RF constraint, respectively. (c) Same as (b) at station ANMO. (d) Ensemble of models at station PFO obtained from the surface-wave inversion without RF constraints. Coloring as in Figure 5. (e) Similar to (d) but the crustal structure has been constrained by the observed RF. (f) & (g) Similar to (d) & (e), but for station ANMO. (Collaborators are V. Levin and J. Park.)

6. References

Artemieva, I.M. and W.D. Mooney, Thermal thickness and evolution of the Precambrian lithosphere: A global study, *J. Geophys. Res., 106*, 16,387-16,414, 2001.

Barmin, M.P., M.H. Ritzwoller, and A.L. Levshin, A fast and reliable method for surface wave tomography, *Pageoph, 158*, 1351-1375, 2001.

Ekström, G., Tromp, J., & Larson, E.W.F., Measurements and global models of surface waves propagation, *J. Geophys. Res., 102*, 8137-8157, 1997.

Goes, S., R. Govers, and P. Vacher, Shallow mantle temperatures under Europe from P and S wave tomography, *J. Geophys. Res., 105*, 11,153-11,169, 2000.

Julia, J., C.J. Ammon, R.B. Herrmann, and A.M. Correig, Joint inversion of receiver function and surface wave dispersion observations, *Geophys. J. Int.*, *143*, 99-112, 2000.

McDonough, W.F. and R.L. Rudnick, Mineralogy and composition of the upper mantle, in: *Ultrahigh-Pressure Mineralogy: Physics and Chemistry of the Earth's Deep Interior* (R.J. Hemley, editor), Reviews in Mineralogy, *37,* Mineralogical Society of America, 1998.

Pollack, H.N., S. J. Hurter, and J.R. Johnson, Heat flow from the Earth's interior: Analysis of the global data set, *Rev. Geophys., 31*, 267-280, 1993.

Ritzwoller, M.H. & Levshin, A.L., Eurasian surface wave tomography: group velocities, *J. Geophys. Res., 103*, 4839-4878, 1998.

Shapiro, N.M. and M.H. Ritzwoller, Monte-Carlo inversion of broad-band surface wave dispersion for a global shear velocity model of the crust and upper mantle, submitted to *Geophys. J. Int.*, 2001.

Trampert, J. & Woodhouse, J.H., Global phase velocity maps of Love and Rayleigh waves between 40 and 150 s period, *Geophys. J. Int., 122*, 675-690, 1995.